Available online at www.sciencedirect.com
SCIENCE DIRECT®
Ultramicroscopy 97 (2003) 171–175
ultramicroscopy
www.elsevier.com/locate/ultramic

Imaging cobalt nanoparticles by amplitude modulation atomic force microscopy: comparison between low and high amplitude solutions

M. Tello[a], A. San Paulo[a], T.R. Rodríguez[a], M.C. Blanco[b], R. García[a,*]

[a] *Instituto de Microelectrónica de Madrid, CSIC, Isaac Newton 8, Tres Cantos, Madrid 28760, Spain*
[b] *Dept. Química-Física, Universidad de Santiago, Santiago de Compostela, Spain*

Received 10 July 2002; received in revised form 17 October 2002

Abstract

In many situations of interest amplitude modulation AFM is characterized by the coexistence of two solutions with different physical properties. Here, we compare the performance of those solutions in the imaging of cobalt nanoparticles. We show that imaging with the high amplitude solution implies an irreversible deformation of the nanoparticles while repeated imaging with the low solution does not produce noticeable changes in the nanoparticles. Theoretical simulations show that the maximum tip–surface force in the high amplitude solution is about 14 nN while in the low amplitude solution is about −4 nN. We attribute the differences in the high and low amplitude images to the differences in the exerted forces on the sample.

Keywords: Atomic force microscope; Amplitude modulation; Nanoparticles

1. Introduction

The characterization and modification of surfaces in air or liquid environments at nanometer scale has experienced a radical transformation since the invention of the atomic force microscope (AFM). Among the different force microscopy techniques, tapping-mode or more generally amplitude modulation AFM stands for its versatility for obtaining high-resolution images of a variety of materials such as DNA molecules, proteins, cells, polymers and nanometer-size particles [1–10]. We have found that as a consequence of the presence of non-linear tip–surface interaction forces, in many cases of interest two different solutions or states coexist with the external parameters [11–14]. Those states give rise to two different imaging regimes, high and low amplitude imaging regimes. In the low amplitude solution the average force per oscillation is negative while in the high amplitude solution the average force is positive. In many cases imaging with the low amplitude solution is performed in the absence of tip–surface contact, while with the high amplitude solution in most of the cases implies tip–surface mechanical contact.

In this letter we compare the performance of those regimes in the imaging of nanometer-size metallic particles. Specifically, we investigate if the

*Corresponding author. Fax: +34-91806-0701.
E-mail address: rgarcia@imm.cnm.csic.es (R. García).

0304-3991/03/$ - see front matter
doi:10.1016/S0304-3991(03)00041-X

apparent height of the particle depends on the imaging regime. We have chosen cobalt nanoparticles deposited on an atomically flat substrate for two reasons. First, they can be thought representative of several nanometer structures usually studied by local probe techniques. Second, due to their solid-like character it is not straightforward to expect a change in size due to the imaging regime.

2. Materials and methods

Cobalt particles were obtained by an electrochemical procedure based on the dissolution of a metallic anode at constant current density. An aprotic solvent (aceonitrile) was employed and tetrabutylammonium acetate was used as stabilizer. The particles present a gaussian distribution in sizes with a maximum value of 4 nm.

The suspension with the particles was sonicated for about 30 min. Then a 10 μl drop was deposited onto a freshly cleaved piece of mica. After 1 min the sample was rinsed in distilled water and dried in a N_2 flow.

The nanoparticles were imaged with a commercial instrument (Nanoscope III; Digital Instruments, CA). Single beam silicon cantilevers (Pointprobe, Nanosensors, Germany) with spring constants in the 25–50 N/m range were used to perform the experiments. The cantilever was oscillated at its free resonance frequency (250–350 kHz depending on the cantilever) with free amplitude A_0 of about 10 nm. All the experiments were performed in air at room temperature and at a relative humidity of about 40%. The images were obtained by scanning the cantilever-tip in a raster fashion across the sample while keeping the oscillation amplitude at a fixed value, set point amplitude (A_{sp}). The images were recorded at a line frequency of 2 Hz (512×512 pixels).

Amplitude dependence on tip–sample separation curves (amplitude curves) were obtained by approaching the tip towards the sample from a distance with negligible tip–sample interaction. The change of the oscillation amplitude was recorded as the tip–sample distance was modified. To minimize tip and/or sample damage during data acquisition, the tip excursion was stopped when the amplitude was reduced by a factor 3 with respect to the free oscillation amplitude. The curves were taken at 2 Hz with a scan size in the 10–50 nm range.

3. Results and discussion

Fig. 1 shows an amplitude curve obtained on the substrate. The amplitude usually decreases with the tip–surface separation. Two step-like discontinuities of about 2.5 nm are observed. Theoretical simulations show that a step-like discontinuity in the amplitude curve represents a transition between the low and high amplitude solutions [11,12]. The transition point depends on the sweep direction. More precisely it depends on the tip's initial conditions that depend on the scanning direction. This dependence gives rise to the presence of a hysteresis loop [14].

The tip–surface imaging regime may be controlled by the feedback or set point amplitude A_{sp}. In this experiment, A_{sp} values above 7.3 nm imply an operation in the low amplitude solution, while values below 3.8 nm set the cantilever in the high amplitude solution. Amplitude values within the 3.8–7.3 nm interval, i.e. belonging to the hysteresis loop, are compatible with both solutions and most likely would produce severe

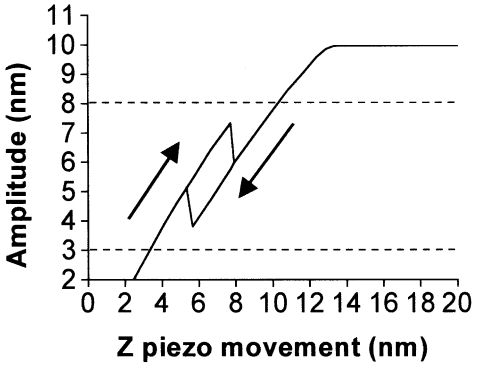

Fig. 1. Amplitude dependence on tip–sample separation curve. The arrows indicate the direction of the acquisition curve. The dashed lines represent the set point values used to perform the experiment. $A_0 = 10$ nm, $f_0 = 350$ kHz.

instabilities in the performance of the microscope.

Fig. 2 shows an image of several nanoparticles obtained with the low amplitude solution. Although the apparent width of the particles is larger than the true width due to tip–sample convolution effects, the AFM gives very precise height measurements.

The experiment proceeds as follows. First an individual cobalt nanoparticle is imaged with the low amplitude solution. Then the set point amplitude is lowered to reach the high amplitude solution and the particle is imaged with this mode. Finally, the amplitude is returned to its initial value (the tip is withdrawn) and the particle is imaged again with the low amplitude solution. The dashed lines in Fig. 1 correspond to the set point amplitudes chosen to perform the imaging of cobalt nanoparticles: the high ($A_{sp} = 8$ nm) and the low amplitude solution set point ($A_{sp} = 3$ nm).

Fig. 3 shows three images of the same nanoparticle and their respective cross-sections taken with the low (Fig. 3(a) and (c)) and the high amplitude (Fig. 3(b)) solutions. The comparison of top view images does not reveal any differences among them. However, the cross-sections of the particle

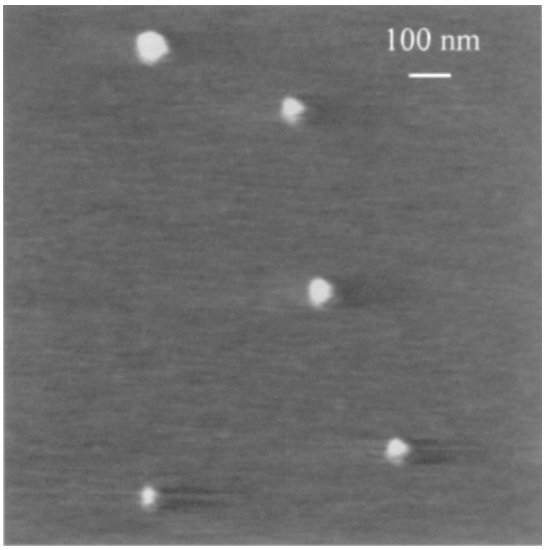

Fig. 2. Amplitude modulation AFM image of several cobalt nanoparticles. The image was taken in the low amplitude interaction regime. $A_0 = 10$ nm, $A_{sp} = 8$ nm.

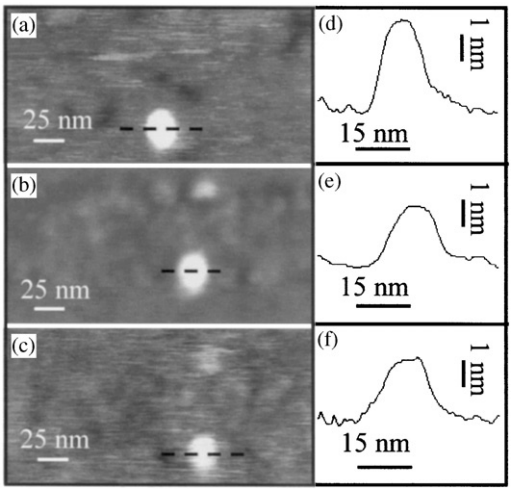

Fig. 3. (a) High-resolution amplitude modulation AFM image of a single cobalt nanoparticle. The image is taken in the low amplitude interaction regime. $A_{sp} = 8$ nm, (b) image of the same nanoparticle in the high amplitude interaction regime. $A_{sp} = 3$ nm, (c) image of the nanoparticle in the low amplitude interaction regime. $A_{sp} = 8$ nm, (d) cross-section along the dashed line in (a), (e) cross-section along the dashed line in (b), (f) cross-section along the dashed line in (c), comparison between (d) and (f) cross-sections reveals the changes in the height of the particle. In all cases $A_0 = 10$ nm, $f_0 = 350$ kHz.

show significant differences. The cross-section corresponding to the first image obtained with the low amplitude solution (Fig. 3(d)), reveals a maximum height of 3.3 nm while the cross-section corresponding to the image with the high amplitude solution shows a height of 2 nm (Fig. 3(e)), which coincides with the cross-section of a subsequent image of the same particle obtained with the low amplitude solution (Fig. 3(f)). The above comparison also illustrates that for those particles imaging with the high amplitude solution produces plastic deformation of the sample.

In order to verify that imaging with the high amplitude solution produces an irreversible deformation of the particles, we have performed a statistical analysis over 40 particles with an initial height in the 3–4 nm range. All of them were successively imaged with the low, high and again low amplitude solutions. The particles were observed with the high amplitude solution for different times ranging from a few seconds to minutes. For a given set point amplitude, the

height decrease was independent of the accumulated contact time between tip and particle.

The height differences observed before and after imaging the particles with the high amplitude solution are presented in Fig. 4. The histogram shows that in most cases, the height of the particle is reduced about 30–40%. The consistent decrease leads to the conclusion that imaging with the high amplitude solution produces an irreversible deformation of the particles.

Two major physical differences distinguish high and low amplitude solutions. First, the high amplitude solution involves tip–surface mechanical contact. Second and closely related to the above, for the same experimental setup the interaction forces present in the high amplitude solution are larger than those in the low amplitude solution. Fig. 5(a) shows the calculation of the oscillation amplitude as a function of the tip–surface separation. Contact forces were simulated by DMT model and long-range attractive forces were described by $F_{vdw} = -HR/6d^2$, where H is the Hamaker constant, R the tip radius and d the tip–sample separation [11]. The values of the Young's modulus, free amplitude, resonance frequency, tip radius and quality factors used in the simulations are similar to those used in the experiment ($E = 1\,\text{GPa}$, $A_0 = 10\,\text{nm}$, $f_0 = 350\,\text{kHz}$, $R = 20\,\text{nm}$, $Q = 400$). Fig. 5(b) shows the corresponding dependence of the maximum force on the amplitude. The force in the high amplitude solution is about three times larger than the force in the low amplitude solution. For the experimental set point values used, the maximum force is $-4\,\text{nN}$ for $A_{sp} = 8\,\text{nm}$ (low amplitude solution), while for $A_{sp} = 3\,\text{nm}$ (high amplitude solution) the maximum force is 14 nN. According to this simulation, the observed deformations produced in the nanoparticles, could be attributed to the differences in the forces involved.

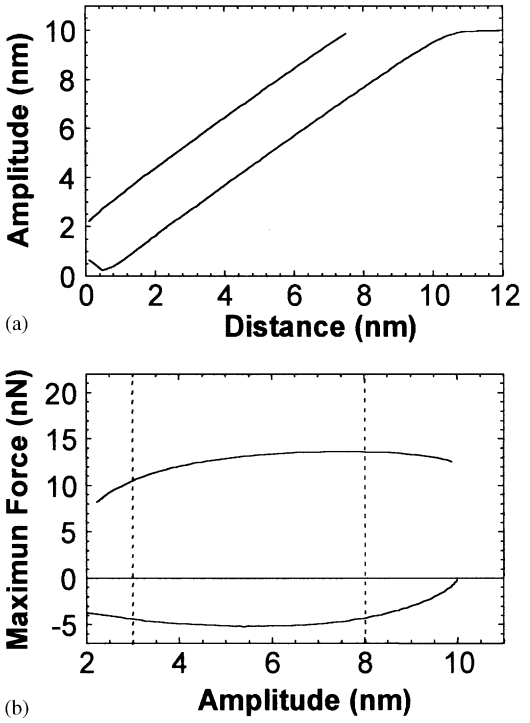

Fig. 5. (a) Theoretical amplitude dependence on tip–sample separation. $E = 1\,\text{GPa}$, $A_0 = 10\,\text{nm}$, $f_0 = 350\,\text{kHz}$, $R = 20\,\text{nm}$, $Q = 400$. (b) Corresponding maximum force dependence on the oscillation amplitude. Dashed lines represent the experimental set point values of the amplitude used to record the images of Fig. 3.

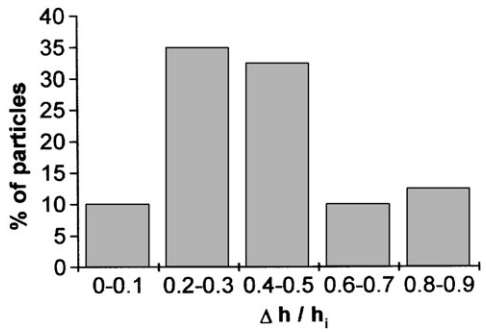

Fig. 4. Histogram of the apparent height differences between first and second imaging in the low amplitude interaction regime. Before second imaging in the low amplitude regime, the nanoparticle was imaged in the high amplitude regime for several seconds. h_i is the initial height and Δh represents the height difference between the first and the second imaging in the low amplitude regime.

The independence of the deformation with the contact time indicates that when the particle is imaged with the high amplitude solution it experiences an inelastic deformation until it reaches a new configuration where it behaves elastically, at least in the range of forces applied in the experiment.

These results are in consistence with previous studies of the physical properties of different nanoparticles that stated that in many cases, nanometer-size particles may be in a non-equilibrium state and/or structure, which may be caused by the method of producing the particles. A continuum model interprets this result indicating that particles below a critical size are stressed beyond their elastic limit and deform to decrease their surface free energy even at temperatures below their melting point [15]. Furthermore, in a wide variety of materials a decrease in solid to liquid transition temperature has been observed with decreasing nanocrystal size [16]. For example, in CdS nanocrystals depressions in the melting point temperature have been described. These depressions can be understood by considering that the surface energy is always lower in the liquid than in the solid phase [17].

Although for the same experimental conditions, a high amplitude solution involves larger forces that the corresponding low amplitude solution, it cannot be generalized that the low amplitude state gives better resolution than the high amplitude state. The deformation depends on the elastic and plastic properties of the sample and on the applied force. For example, we have not observed differences in the dimensions of several III–V semiconductor systems after imaging with the high amplitude solution. On the other hand, lateral resolution depends on sample deformation as well as on tip–surface separation [18].

4. Conclusion

In this paper we have compared the performance of low and high amplitude solutions of amplitude modulation AFM for the imaging of Co nanoparticles. Repeated imaging with a low amplitude solution does not produce any changes in the height and width of the particles. On the other hand, imaging the particles with a high amplitude solution produces irreversible modification in their height. Those changes are associated with the maximum force exerted by the tip on the particle. For standard operating conditions, high amplitude solutions imply maximum forces several times larger than those corresponding to low amplitude solutions. The deformation of the particles when experiencing forces of tens of nN may indicate that their structure does not correspond to the equilibrium.

The above experiments emphasize the role of amplitude curves for determining the experimental parameters that minimize tip–surface forces while optimizing spatial sensitivity.

Acknowledgements

This work was supported by the Dirección General de Enseñanza Superior e Investigación (PB98-0471).

References

[1] C. Bustamante, D. Keller, Phys. Today 48 (1995) 33.
[2] M. Bezanilla, B. Drake, E. Nudler, M. Kashev, P.K. Hansma, H.G. Hansma, Biophys. J. 67 (1994) 2454.
[3] D.D. Dunlap, A. Maggi, M.R. Soria, L. Monaco, Nucleic Acids Res. 25 (1997) 3095.
[4] Y.L. Lyubchenko, L.S. Shlyakhtenko, Proc. Natl. Acad. Sci. USA 94 (1997) 496.
[5] M. Stark, C. Möller, D.J. Müller, R. Guckenberger, Biophys. J. 80 (2001) 3009.
[6] A. San Paulo, R. García, Biophys. J. 78 (2001) 1599.
[7] V. Vié, M.C. Giocondi, E. Lesniewska, E. Finot, J.P. Goudonnet, C. Le Grimellec, Ultramicroscopy 82 (2000) 279.
[8] G. Reiter, G. Castelain, J.U. Sommer, A. Röttele, T. Thurn-Albrecht, Phys. Rev. Lett. 87 (2001) 2261.
[9] T. Junno, K. Deppert, L. Montelius, L. Samuelson, Appl. Phys. Lett. 66 (1995) 3627.
[10] R. García, M. Calleja, H. Rohrer, J. Appl. Phys. 86 (1999) 1898.
[11] R. García, A. San Paulo, Phys. Rev. B 60 (1999) 4961.
[12] R. García, A. San Paulo, Phys. Rev. B 61 (2000) R13381.
[13] M. Marth, D. Maier, J. Honerkamp, R. Brandsch, G. Bar, J. Appl. Phys. 85 (1999) 7030.
[14] A. San Paulo, R. García, Phys. Rev. B 66 (2002) 041406(R).
[15] E.L. Nagaev, Sov. Phys. Usp. 35 (1992) 747.
[16] A.P. Alivisatos, J. Phys. Chem. 100 (1996) 13226.
[17] A.N. Goldstein, C.M. Echer, A.P. Alivisatos, Science 256 (1992) 1425.
[18] R. García, R. Pérez, Surf. Sci. Rep. 47 (2002) 197.